



Published in final edited form as:

*Clin Cancer Res.* 2014 May 1; 20(9): 2375–2387. doi:10.1158/1078-0432.CCR-13-1415.

## Mesenchymal Stem Cells from Human Fat Engineered to Secrete BMP4 are Non-Oncogenic, Suppress Brain Cancer, and Prolong Survival

Qian Li<sup>1</sup>, Olindi Wijesekera<sup>1</sup>, Sussan J. Salas<sup>2</sup>, Joanna Y. Wang<sup>1</sup>, Mingxin Zhu<sup>1,3</sup>, Colette Aprhys<sup>1</sup>, Kaisorn L. Chaichana<sup>1</sup>, David A. Chesler<sup>1,4,5</sup>, Hao Zhang<sup>6</sup>, Christopher L. Smith<sup>7</sup>, Hugo Guerrero-Cazares<sup>1</sup>, Andre Levchenko<sup>8,\*</sup>, and Alfredo Quinones-Hinojosa<sup>1,\*</sup>

<sup>1</sup>Department of Neurosurgery and Oncology, Johns Hopkins University School of Medicine, Baltimore, Maryland, USA

<sup>2</sup>Department of Neurosurgery, Jefferson Medical College, Philadelphia, Pennsylvania, USA

<sup>3</sup>Department of Neurosurgery, Tongji Hospital, Tongji Medical College, Huazhong University of Science & Technology, Wuhan, Hubei, People's Republic of China

<sup>4</sup>Department of Neurosurgery, University of Maryland, Baltimore, Maryland, USA

<sup>5</sup>Division of Pediatric Neurosurgery, Johns Hopkins University School of Medicine, Baltimore, Maryland, USA

<sup>6</sup>Department of Molecular Microbiology and Immunology, Bloomberg School of Public Health, Johns Hopkins University, Baltimore, Maryland, USA

<sup>7</sup>Department of Biomedical Engineering, Johns Hopkins University School of Medicine, Baltimore, Maryland, USA

<sup>8</sup>Department of Biomedical Engineering, Yale University, New Haven, Connecticut, USA

### Abstract

**Purpose**—Glioblastoma (GBM) is the most common adult primary malignant intracranial cancer. It is associated with poor outcomes due to its invasiveness and resistance to multimodal therapies. Human adipose-derived mesenchymal stem cells (hAMSCs) are a potential treatment because of their tumor tropism, ease of isolation, and ability to be engineered. In addition, bone

---

\* **Corresponding Authors** Alfredo Quinones-Hinojosa, Department of Neurosurgery, Johns Hopkins University, 1550 Orleans St, CRB-II, Room 247, Baltimore, MD 21201. Phone: 410-502-2869, Fax: 410-502-7559, aquinon2@jhmi.edu Andre Levchenko, Department of Biomedical Engineering, Yale University, P.O. Box 208260, New Haven, CT 06520. Phone: 203-432-4795, andre.levchenko@yale.edu.

Conflict of Interest

The authors declare no conflict of interest and no financial disclosures.

Author Contributions

**Conception and design:** QL, SJS, HGC and AQH.

**Acquisition of data:** QL, OW, SJS, JYW, MZ and KLC.

**Analysis and interpretation of data:** QL, OW, SJS, JYW and MZ.

**Writing, review and/or revision of the manuscript:** QL, OW, JYW and AQH wrote the manuscript; KLC, HGC, DAC and AL edited the manuscript.

**Administrative, technical, or material support:** HZ and CLS.

morphogenetic protein 4 (BMP4) has tumor-suppressive effects on GBM and GBM brain tumor initiating cells (BTICs), but is difficult to deliver to brain tumors. We sought to engineer BMP4-secreting hAMSCs (hAMSCs-BMP4) and evaluate their therapeutic potential on GBM.

**Experimental Design**—The reciprocal effects of hAMSCs on primary human BTIC proliferation, differentiation, and migration were evaluated *in vitro*. The safety of hAMSC use was evaluated *in vivo* by intracranial co-injections of hAMSCs and BTICs in nude mice. The therapeutic effects of hAMSCs and hAMSCs-BMP4 on the proliferation and migration of GBM cells as well as the differentiation of BTICs, and survival of GBM-bearing mice were evaluated by intracardiac injection of these cells into an *in vivo* intracranial GBM murine model.

**Results**—hAMSCs-BMP4 targeted both the GBM tumor bulk and migratory GBM cells, as well as induced differentiation of BTICs, decreased proliferation, and reduced the migratory capacity of GBMs *in vitro* and *in vivo*. In addition, hAMSCs-BMP4 significantly prolonged survival in a murine model of GBM. We also demonstrate that the use of hAMSCs *in vivo* is safe.

**Conclusions**—Both unmodified and engineered hAMSCs are non-oncogenic and effective against GBM, and hAMSCs-BMP4 are a promising cell-based treatment option for GBM.

### Keywords

glioblastoma; human adipose-derived mesenchymal stem cells; brain tumor initiating cells; BMP4

---

### Introduction

Glioblastoma (GBM) is the most common and aggressive malignant primary intracranial neoplasm in adults (1). The median survival for patients with GBM is approximately 14.6 months, despite aggressive combinatorial treatment (1). The malignant nature of GBM and its ability to resist multimodal treatments have been attributed to its highly proliferative and migratory ability as well as its heterogeneous cell composition (2-6). This heterogeneity is theorized to be due to a small population of stem-like progenitor cells called brain tumor initiating cells (BTICs) (2-6). BTICs are highly resistant to chemotherapy and radiation therapy, and may underlie the high recurrence rate and treatment failure observed in GBM patients (2-6). Therefore, therapies directly targeting BTICs might be more effective than current therapies.

Mesenchymal stem cells (MSCs) are clonally expansive with the capacity to differentiate into osteocytes, adipocytes, and chondrocytes under specific *in vitro* stimuli (7, 8). Commonly used types of MSCs are bone marrow-derived MSCs (BM-MSCs) and human adipose-derived MSCs (hAMSCs) (7, 9). MSC's intrinsic ability to home to tumors, ease of isolation from various tissues, and ability to readily expand *in vitro* make them attractive candidates to deliver specific, targeted cancer therapeutics (9-15). The effects of MSCs on tumor cells *in vivo*, however, remain incompletely characterized, and seem to depend heavily on cancer type and source of MSCs (14, 15). Unlike BM-MSCs, hAMSCs are easier to obtain, more genetically and morphologically stable in long-term culture, have a lower senescence ratio, and have a greater proliferative capacity (7, 9). Of the limited number of studies that have evaluated the effect of hAMSCs on commercial GBM cell lines, some found these cells reduced tumor recurrence and had an overall tumor-suppressive effect (11,

16, 17). However, there have also been reports of MSCs transforming into tumor associated fibroblasts (TAFs), which can potentially support tumor growth and promote a malignant phenotype (18-20). Yet, no studies have evaluated the effects of hAMSCs on human BTICs *in vivo* with a primary cell line. Furthermore, no studies have reported the changes that may occur in hAMSCs after they interact with human BTICs.

Due to their capability to target GBM cells, hAMSCs can be used to deliver therapeutic agents to GBM (9, 21-23). Bone morphogenetic protein 4 (BMP4) is a potential therapeutic agent that has been shown to have an anti-proliferative effect on neural progenitor cells (24-28), and, more recently, has been shown to significantly decrease the proliferation of stem-like, tumor-initiation precursors of GBMs as well as drive the differentiation of these cells towards a predominantly glial fate (29). These findings make BMP4 a promising treatment for GBM, but no studies thus far have investigated its therapeutic potential or its ability to be delivered via stem cells (29). The goals of this study were to investigate the interaction between BTICs and hAMSCs-BMP4 and the reciprocal effects of each cell type on the other's proliferation, differentiation, and migration. Furthermore, we investigated the effect of hAMSCs-BMP4 on survival in a mouse model of GBM. These interactions are paramount to understanding the utility of hAMSCs and BMP4 to treat GBM in human clinical trials.

## Material and Methods

### Cell lines

Early passage hAMSCs and BTIC cultures were used and authenticated by Johns Hopkins Genetic Resources Core Facility. hAMSCs (Invitrogen, R7788-115) were cultured in MesenPRO complete media (1% Antibiotic/Antimycotic (Invitrogen, 15240-062), 1% Glutamax (GIBCO, 35050-061), 1 vial of MesenPRO RS growth supplement (GIBCO, 12748-018), and MesenPRO RS basal media (GIBCO, 12747-010)). Human BTIC cultures (276 and 612) were obtained from intraoperative tissue (as approved by Johns Hopkins Institutional Review Board) and cultured in laminin-coated flasks (Sigma, L2020, 1  $\mu\text{g}/\text{cm}^2$ ) with stem cell media (30). As previously validated and shown by our group, the human BTIC cultures are able to form oncospheres, are multipotential, and form tumors when implanted into animal models (30). To evaluate the tumorigenic capacity of BTICs *in vivo*, BTIC line 276 was injected intracranially in mice by our group resulting in the formation of solid tumors, while 612 formed diffuse tumors (30, 31). The molecular subtype of BTIC culture 276 is mesenchymal and 612 is proneural, which was determined using a metagene score based approach for subtype designation, assessing four mesenchymal and two proneural genes using a microfluidics based qPCR assay (32). Commercial U87 cells (ATCC, HTB-14) were cultured in DMEM media with 10% FBS.

### Retroviral production, lentiviral production, and infection

To induce the expression of BMP4 in hAMSCs, an MFG-based retroviral vector system was combined with a BMP2/4 hybrid (33). To identify hAMSCs and BTICs in our *in vitro* co-culture and *in vivo* mouse experiments, we transduced these cells with lentiviral vectors coding for GFP, td-tomato, or GFP/bioluminescent proteins. Viral vectors were packaged

from HEK293 cells. After collection and concentration, hAMSCs (hAMSCs-Vector, hAMSCs-BMP4, GFP/ bioluminescent-hAMSCs, and td-tomato-hAMSCs) and BTICs (GFP-276 and GFP-612) were infected and sorted by a MoFlo cytometer (Beckman Coulter, Miami, FL, USA).

### Co-injection *in vivo* studies

To investigate the effect and the safety of co-injected hAMSCs on GBM cell proliferation *in vivo*, 6-8 week NOD/SCID mice were stereotactically injected with  $0.5 \times 10^6$  GFP-276 (n=5),  $0.5 \times 10^6$  td-tomato-hAMSCs (n=5),  $0.5 \times 10^6$  GFP-276 mixed with  $0.5 \times 10^6$  td-tomato-hAMSCs (co-injection) (n=5), and  $1.0 \times 10^6$  GFP/bioluminescent-hAMSCs into the right striatum (L: 1.34 mm, A: 1.5 mm, D: 3.5 mm) (n=5). Following injection, mice in the GFP/bioluminescent hAMSC group were imaged using an IVIS small animal imaging system (PerkinElmer) at different time periods (7, 14, and 28 days post injection). After 4 weeks, animals were euthanized and perfused with 4% PFA. Brains were extracted, cryo-sectioned, and immunostained for human nuclei (Millipore, MAB4383). To quantify tumor area, tumor mass was outlined based on DAPI staining and calculated using Image J. To quantify GBM cell migration, the distance from the tumor margin, determined by DAPI staining, to each human nuclei+/DAPI+/td-tomato- cell was quantified. A blinded observer performed all counting.

### hAMSCs-BMP4 *in vivo* studies

To determine the effect of hAMSCs-BMP4 on the malignancy of orthotopic GBM tumors *in vivo*,  $1 \times 10^6$  BTIC 276 were suspended in 2  $\mu$ l PBS and stereotactically injected into the right striatum (L: 1.34 mm, A: 1.5 mm, D: 3.5 mm) of immunosuppressed nude mice. Two weeks post-injection,  $0.5 \times 10^6$  GFP-hAMSCs-Vector (n=7), GFP-hAMSCs-BMP4 (n=5), or equal volume of PBS (n=5, 100  $\mu$ l) were systemically injected into the left cardiac ventricle (34). After 2 weeks, the mice brains were perfused, fully cryo-sectioned at a 10 micron thickness, and immunostained for GFP, BMP4 (Abcam, ab93939), Ki67 (Thermo, RM-9106-s1), Nestin (Abcam, ab5922), Tuj1, GFAP, TNF- $\alpha$  (Abcam, ab6671), VEGF (Abcam, ab46154), and human nuclei. Tumor mass was outlined and cell number of positive staining inside the tumor mass was counted and normalized relative to DAPI inside the tumor bulk. The ratio of Ki67+/DAPI was used to measure proliferation; Nestin+/DAPI, Tuj1+/DAPI, and GFAP+/DAPI to measure differentiation; and TNF- $\alpha$ /DAPI and VEGF+/DAPI to measure tumor necrosis and angiogenesis. Immunostaining for Nestin was used as a BTIC marker, as this has been validated in several studies (35, 36). To quantify GBM cell migration, human nuclei antibodies were used. Tumor mass was outlined by DAPI and the center of tumor mass was calculated using Image J. The distance from the center of tumor mass to each human nuclei+/DAPI+/GFP- cell was quantified based on 110-250 cells per group. A blinded observer performed all counting. 41, 38, and 41 slides have been analyzed in PBS, hAMSCs-Vector, and hAMSCs-BMP4 groups, respectively. All *in vivo* procedures were approved by the Johns Hopkins University Animal Care and Use Committee.

## Survival study

To determine the effect of hAMSCs-BMP4 on the survival of orthotopic GBM tumors-bearing mice *in vivo*,  $0.5 \times 10^6$  U87 were suspended in 2  $\mu$ l PBS and stereotactically injected into the right striatum (L: 1.34 mm, A: 1.5 mm, D: 3.5 mm) of immunosuppressed nude mice. Ten days post-injection,  $0.5 \times 10^6$  hAMSCs-Vector (n=7), GFP-hAMSCs-BMP4 (n=5), or equal volume of PBS (n=10, 100  $\mu$ l) were systemically injected into the left cardiac ventricle. Mice were followed for 125 days to monitor survival. A Kaplan-Meier survival analysis was performed with results reported as the median and mean survival times with a 95% confidence interval. The statistical difference between the three conditions was determined by log rank analysis.

## Statistical analysis

Results are reported as mean  $\pm$  S.E.M. Comparisons were done using two-way ANOVA for MTS assays, one-way ANOVA (Kruskal-Wallis test follow up an Dunns post test) for transwell and nanopattern assays, A Kaplan-Meier survival analysis was performed with results reported as the median survival times with a 95% confidence interval. The statistical difference between the three conditions was determined by log rank analysis, and *t*-tests (Mann-Whitney) for other experiments using GraphPad Prism 5 (La Jolla, CA) software. Statistical significance was defined as  $p < 0.05$ .

## Results

### hAMSCs-BMP4 decrease migration of BTICs by reducing both migration and migration speed *in vitro*

Prolific migration of GBM cells and BTICs greatly contributes to the mortality of the disease. Human MSCs have been shown to have intrinsic tumor suppressive affects in some models (37), and the effects of hAMSCs and BMP4 on GBM and BTIC migratory capacity has not yet been evaluated. Thus, we investigated whether unmodified hAMSCs and BMP4 secreting-hAMSCs (hAMSCs-BMP4) could affect the migratory capabilities of BTICs *in vitro*.

hAMSCs-BMP4 cells were able to synthesize and release BMP4 as shown by Western blots performed with cell lysates and conditioned media from hAMSCs-BMP4 and hAMSCs-Vector. The majority of mature BMP4 is extracellular, and there is no visible mature BMP4 in the hAMSCs-Vector cells (Fig.1A). As shown in Supplementary Figure 1A,  $1 \times 10^6$  hAMSCs-BMP4 cells secrete approximately 74 ng after 3 days of culturing.

Using *in vitro* Boyden chamber transwell assays, the effect of hAMSCs-Vector, hAMSCs-BMP4, and an exogenous 50 ng/ml BMP4 dose on BTIC migration was assessed (Fig. 1C). Conditioned media from empty vector infected hAMSCs (hAMSC-Vector-CM), hAMSCs-BMP4 (hAMSC-BMP4-CM), and BMP4-supplemented media resulted in a 2-fold decrease in the number of migrating BTICs (Fig. 1C,  $p < 0.001$ ). However, there were no significant differences between these three treatments ( $p > 0.05$ ). Similar findings were seen when using a different BTIC line (BTIC 612) (Supplementary SFig. 1B-D).

To assess the effects of hAMSCs and BMP4 on BTIC migration speed, a nanopattern chamber was used (Fig. 1D). BTIC migration speed decreased when cultured in hAMSC-Vector-CM and hAMSC-BMP4-CM, as well as in the BMP4 treatment group (50 ng/ml) by almost 2-fold for both 612 (Fig. 1E,  $p<0.01$ ) and 276 (Supplementary SFig. 1E-F,  $p<0.05$ ) BTICs. There was no significant difference in the ability of hAMSC-Vector-CM, hAMSC-BMP4-CM, and BMP4 to decrease the migration speed of BTICs (Fig. 1E,  $p>0.05$ ).

### **hAMSCs-BMP4 decrease proliferation of BTICs *in vitro***

Another key feature underlying the malignant nature of GBM is its capacity for unlimited and rapid proliferation. Previous studies have demonstrated the effects of BMP4 in reducing the proliferative capabilities of BTICs (29), but there are none that report the effects of hAMSCs on BTIC proliferation. Therefore, MTS (to test cell viability and proliferation as a function of time) and EdU assays (to examine cell proliferation at specific time points) were used to evaluate the effects of BMP4, hAMSC conditioned media, and hAMSC-BMP4 conditioned media on BTICs. Using the MTS assay, hAMSC-CM treatment resulted in no statistically significant difference in proliferation between the hAMSC-CM and the control groups during the first 10 days ( $p>0.05$ ) (Fig. 2A). However, hAMSC-CM decreased proliferation of both 276 (Fig. 2A) and 612 BTICs (Supplementary SFig. 2A) significantly at day 13 ( $p<0.05$ ). In comparison, exogenous BMP4 (100 ng/ml) demonstrated a significant decrease in BTIC proliferation after day 7 for 276 (Fig. 2B) and at day 13 for 612 (Supplementary SFig. 2B) ( $p<0.01$ ). To verify these results and further investigate whether cell-cell interactions between hAMSCs and BTICs (co-culture EdU assay) could affect the proliferation of BTICs, we co-cultured hAMSCs with BTICs and found the proliferation of 276 cells decreased significantly (Fig. 2C and Supplementary SFig. 2C, 3-fold decrease at both day 5 and day 13,  $p<0.05$ ); Furthermore, when treated with exogenous BMP4 (50 ng/ml) for 48 hours, proliferation of 276 cells decreased significantly (Fig. 2D, 30% decreased,  $p<0.05$ ). BTIC proliferation also decreased significantly when co-cultured with hAMSCs-BMP4 (Fig. 2E, for 276, 2-fold decrease at 5 days,  $p<0.001$ ). Similar effects were seen using the 612 BTIC line (Supplementary SFig. 2D-E). These experiments demonstrate that BMP4 and hAMSCs-BMP4 decrease the proliferation of BTICs effectively *in vitro*, and that unaltered hAMSCs can also decrease the proliferation of BTICs via secreted proteins and cell-cell contact.

### **hAMSCs-BMP4 induce differentiation of BTICs *in vitro***

BTICs appear to underlie the ability for GBM migration and proliferation; inducing the differentiation of BTICs may attenuate the malignant features of GBM. Previous studies have shown that BMP4 can induce differentiation of BTICs (29). We verified this in our experimental system and further examined the effects of hAMSC-secreted molecules and hAMSCs-BMP4 on BTIC differentiation potential. The ability of hAMSCs and hAMSCs-BMP4 to induce differentiation of BTICs was examined. BTICs were cultured in different media conditions and immunofluorescent staining was used to identify different lineage markers (Fig. 3A). Compared to the negative control (undifferentiated BTICs, cultured in stem cell media), the percentages of Tuj1+/DAPI and GFAP+/DAPI were both significantly increased in hAMSC-Vector-CM, hAMSC-BMP4-CM, and BMP4 treatment groups as well as in the positive control group (differentiated BTICs, cultured in stem cell media+10%

FBS) for 276 ( $p < 0.001$ ) (Fig. 3B). Similar results were obtained using 612 (Supplementary SFig. 3). Although the BTICs express GFAP or Tuj1 proteins, we observed many double positive cells, which would indicate maturation of the cells. However, the BTICs have not begun to take on the classic neuronal and astrocytic morphologies, which could be due to the timing of our experiments.

### **hAMSCs remain multipotent and retain their proliferation capacity when exposed to BTIC-secreted factors or are transduced with BMP4 *in vitro***

To consider hAMSCs as delivery vehicles in GBM treatment, they must retain certain intrinsic characteristics when exposed to GBM or GBM tumor environment. The exposure of hAMSCs to BTIC-CM did not alter their proliferation capacity via MTS assay (276-CM were used in Fig. 4A,  $p > 0.05$ ). This result was replicated when the effects of BTIC-hAMSC cell-cell interaction was examined by EdU co-culture assays (Fig. 4B). The percentage of proliferating hAMSCs when cultured alone was not significantly different compared to those co-cultured with BTICs (32% vs. 26%,  $p > 0.05$ ). These results were replicated using BTIC line 612 (Supplementary SFig. 4A-B).

The ability of hAMSCs to remain multipotent upon exposure to BTIC-secreted factors was examined using differentiation assays. Similar to the negative control (undifferentiated hAMSCs), hAMSCs incubated in 276 BTIC-CM stained negative for adipogenesis (first row of Fig. 4D) and osteogenesis (second row of Fig. 4D). Although there was presence of Masson's Trichrome staining in the 276-CM and negative control groups, the positive control group (differentiated hAMSCs) had appreciably more staining (third row of Fig. 4D). Concurrently, mRNA expression levels were used to quantify adipogenic (*CEBPA* and *LPL*), osteogenic (*OP* and *ALPL*), and chondrogenic (*SOX9*) differentiation. Normalized and compared to the negative control group (undifferentiated hAMSCs), mRNA levels of all markers in the CM group were not significantly different ( $p > 0.05$ ) (Fig. 4C). Similar results were obtained using 612 CM (data not shown).

Additionally, the proliferation, differentiation, and migration of hAMSCs-Vector and hAMSCs-BMP4 were examined to evaluate if retroviral modification altered hAMSC characteristics. In regards to proliferation, the effect of BMP4 on hAMSC proliferation was examined as a positive control. BMP4 significantly reduced the proliferation of hAMSCs by approximately 10% in a time-dependent manner (Fig. 4E,  $p < 0.05$ ). BMP4-secreting hAMSCs also showed a decrease in proliferation when compared to hAMSCs-Vector suggesting an auto- or paracrine effect (Fig. 4F,  $p < 0.05$ ). In regards to differentiation, the differentiation potential of hAMSCs was not altered when treated with exogenous BMP4 or when they were induced to express BMP4 (hAMSCs-BMP4; Fig. 4G). In regards to migration, hAMSCs-Vector and hAMSCs-BMP4 cells migrated towards BTIC-CM more than to control media indicating their preserved GBM tropism (276, Fig. 4H-I,  $p < 0.05$ ; 612, data not shown,  $p < 0.05$ ). Engineered hAMSCs respond to and migrate towards factors secreted by BTICs, with a more pronounced response seen in hAMSCs-BMP4 (2-fold increase in hAMSCs-BMP4 group, and 1.1-fold increase in hAMSCs-Vector group), suggesting that modified hAMSCs might result in a more targeted therapy. BMP4 transduction may also enhance the migration ability of hAMSCs *in vivo*.

### **hAMSCs are not tumorigenic when exposed to BTICs *in vitro* and *in vivo***

The potential of hAMSCs to undergo malignant transformation into TAFs and undergo subsequent increased tumor growth and migration when exposed to BTIC secreted factors was examined. The expression of TAF markers (increased expression levels of vimentin and ACTA2) was evaluated by Western blot and real-time RT-PCR. There were no significant differences in protein levels up to 2 weeks, and there was even less ACTA2 expression after 3 weeks of culturing in BTIC-CM (276, Fig. 5A; and 612, data not shown). Similarly, there were no significant differences in mRNA levels after 1-3 weeks of culturing in BTIC-CM (276,  $p>0.05$ , shown in Fig. 5B; 612,  $p>0.05$ , data not shown). Moreover, there were no differences in vimentin or ACTA2 immunofluorescence staining when exposed in BTIC-CM after 3 weeks (data not shown). hAMSCs endogenously express vimentin and ACTA2, and exposure to BTICCM did not increase expression of these markers.

The proliferative capacity and survival time of hAMSCs was subsequently examined *in vivo* after intracranial co-injection of BTICs and hAMSCs (Fig. 5C). The GFP/bioluminescent hAMSCs (GFP-hAMSCs) group was imaged from 7 to 28 days post-injection. The bioluminescent signal declined dramatically after 14 days and remained virtually non-existent *in vivo* (Fig. 5E). There was no observable GFP signal (hAMSCs) in the GFP-hAMSCs group at 3 months *in vivo* (Supplementary SFig 5). Additionally, there was no observable td-tomato (hAMSCs) in the co-injection group (data not shown). Even after staining for GFP (data not shown) and human nuclei, co-localization of human nuclei and GFP was only found in the GFP-276 and co-injection groups and no signals in GFP-hAMSCs or PBS groups (data not shown). After 4 weeks, the co-injection group had a smaller mean tumor area of 135,700  $\mu\text{m}^2$  as compared to GFP-BTIC group, with a mean tumor area of 209,800  $\mu\text{m}^2$  ( $p=0.0189$ ) (Fig. 5D). When measuring individual cell distance from the tumor margin, there was no significant difference between the BTICs-only and co-injection groups ( $p=0.3442$ ) (Supplementary SFig 5C). Additionally, as shown in Figure 5F, tumors in the BTIC group appear larger than the co-injection group, suggesting presence of additional hAMSCs does not contribute to rampant tumor progression *in vivo*.

### **hAMSCs-BMP4 increase the median survival time of GBM bearing mice, drive differentiation, and decrease proliferation and migration of GBM cells *in vivo***

To examine the effects of hAMSCs-BMP4 on GBM cell proliferative capacity and migratory ability, and on stem-ness of BTICs *in vivo*, a mouse model of GBM was created as described previously by our group (38). In this model, hAMSCs-Vector ( $n=7$ ), hAMSCs-BMP4 ( $n=5$ ), or PBS ( $n=5$ ) were administered via cardiac injection after GBM tumor formation (Fig. 6F). As shown in Figure 6A, there was only BMP4 (human specific antibodies) seen in mice injected with hAMSCs-BMP4. Subsequently, GFP staining confirmed the homing of the hAMSCs-Vector and hAMSCs-BMP4 groups to the tumor bulk. As shown in Figure 6A, C-D, hAMSCs-Vector and hAMSCs-BMP4 migrated to the tumor bulk (defined by DAPI density). Interestingly, in only the hAMSCs-BMP4 group, GFP signals were found around migratory BTICs (defined by Nestin+ cells not part of the tumor bulk) (Fig. 6B). Human specific Ki67 staining was used to assess proliferation, and no Ki67+ cells were observed co-localizing with GFP+ hAMSCs (Fig. 6C). To quantify the effect of hAMSCs-Vector and hAMSCs-BMP4 on GBM cell proliferation, Ki67+ cells were



normalized with corresponding DAPI+ cells in the tumor mass. There was a 2-fold decrease in the ratio of Ki67+/DAPI in the hAMSCs-BMP4 group compared to both the PBS group and hAMSCs-Vector group (Fig. 6C,  $p<0.05$ ). Additionally, immunofluorescence staining for TNF- $\alpha$  and VEGF were performed to investigate characteristics of malignant tumors (TNF- $\alpha$  is a marker for necrosis, and VEGF is a proangiogenic molecule; TNF- $\alpha$  and VEGF secretion are also known associated with TAFs). As seen in Supplementary SFig.6, there were decreased TNF- $\alpha$  and VEGF staining in the hAMSCs-Vector and hAMSCs-BMP4 groups (2-fold of decrease,  $p<0.05$ )

The ability of hAMSCs-Vector and hAMSCs-BMP4 to induce differentiation of BTICs *in vivo* were evaluated by staining cells for Nestin, GFAP, and Tuj1. There was an increased number of Nestin+ cells in the PBS group, and an increased number of GFAP+ and Tuj1+ cells in the hAMSCs-Vector and hAMSCs-BMP4 groups ( $p<0.05$ ) (Fig. 6D). We also observed that hAMSCs-BMP4 can decrease the number of Nestin+ cells compared to the hAMSCs-Vector group.

In addition, to determine if hAMSCs-Vector and hAMSCs-BMP4 can affect the migration of GBM cells *in vivo*, the tumor bulk was outlined utilizing DAPI staining. The average distance of GBM cells (human nuclei+/DAPI+/GFP- cells) that migrated from the center of tumor bulk was calculated based on human nuclei staining (Fig. 6E). As shown in Figure 6E, hAMSCs-Vector and hAMSCs-BMP4 both inhibited the migratory ability of GBM cells significantly ( $p<0.001$ ). Additionally, as compared to the hAMSCs-Vector group, hAMSCs-BMP4 significantly decreased the migration of GBMs (Fig. 6E,  $p<0.001$ ).

To investigate if hAMSCs-Vector and hAMSCs-BMP4 can affect the survival of GBM bearing mice,  $0.5 \times 10^6$  U87 cells were stereotactically injected into immunosuppressed nude mice. Ten days post-injection,  $0.5 \times 10^6$  hAMSCs-Vector ( $n=7$ ), GFP-hAMSCs-BMP4 ( $n=5$ ), or equal volume of PBS (100  $\mu$ l,  $n=10$ ) were systemically injected into the left cardiac ventricle. Mice were followed for 125 days to monitor survival. As shown in Figure 6G, the median survival of mice treated with hAMSCs-BMP4 (undefined) was significantly greater than that of mice treated with hAMSCs-Vector ( $p=0.01$ ) (76 days) and control mice ( $p=0.002$ ) (52 days). There was no significant difference between the PBS and hAMSCs-Vector group ( $p=0.09$ ).

## Discussion

Glioblastoma (GBM) is the most common and aggressive malignant primary intracranial neoplasm in adults, with a median survival of approximately 14.6 months despite combinatorial treatments of surgical resection, chemotherapy, and radiotherapy (39). GBM has heterogeneous genetic alterations in pathways associated with proliferation, survival, invasion, and angiogenesis. GBM cells are known to use white matter tracts and microvasculature basement membranes to migrate long distances, making complete surgical resection of the tumor difficult, almost inevitably leading to recurrence (40). The well-known GBM molecular subtype classifications are proneural, neural, classical, and mesenchymal (41). The two primary glioblastoma cell lines used in this study, 276 and 612, belong to mesenchymal and proneural subtypes, respectively. hAMSCs-BMP4 treatment

was able to attenuate malignant tumor characteristics of two different subtypes of GBM in this study, reinforcing the therapeutic effect of hAMSCs-BMP4 in potential future clinical trials.

Although human MSCs have been manipulated to express a wide variety of anticancer therapeutic factors due to their tropism towards inflammation and tumor cells (17, 42-44), the effects of hAMSCs on GBM and BTICs have not been fully described. This study was the first to find that hAMSCs inhibit proliferation and induce differentiation of BTICs, as well as confirm that hAMSCs decrease the migration of BTICs *in vitro*. Furthermore, hAMSCs can induce differentiation, reduce proliferation and migration, and may even diminish angiogenesis of GBM *in vivo* when injected intracardially. However, when intracranially co-injected with BTICs, we did not observe a difference in the extent of cell migration *in vivo*, but we did find a reduction in tumor size. These results indicate that hAMSCs can have intrinsic anti-tumor effects and are promising for GBM treatment. However, we found that unmodified hAMSCs have a limited effect on inhibiting GBM cell proliferation and survival, and they can only track GBM tumor bulk but lack the ability to home to migratory GBM cells *in vivo*. Enhancement of the hAMSCs by engineering them to deliver specific agents may augment their anticancer effects (37).

BMPs are known to play a role in the differentiation of adult neural stem cells into different mature cell types (45, 46). Recently, BMP4 has been shown to reduce GBM tumor burden *in vivo* and improve survival in a mouse model of GBM by potentially reducing the frequency of symmetric cell divisions or by blocking proliferation and inducing differentiation of BTICs (29). One of the challenges to effective treatment of GBM is the targeting of BTICs, which appear to underlie the ability of the tumor to recur (2). BMP4 is an ideal therapeutic candidate because of its affect on BTICs; however, optimizing its delivery is critical (47). Aside from local delivery with polyacrylic beads (29), there are no reports describing stem cell-based vehicles for BMP4 delivery. The goal of the *in vitro* experiments was to demonstrate the potential therapeutic effects hAMSCs-BMP4 have on GBM. We found that BMP4 treatment, whether exogenously administered or released by genetically modified hAMSCs, can decrease the proliferation of BTICs and make BTICs commit to mature lineages *in vitro* and *in vivo*. Most of these effects are also observed with unmodified hAMSCs, but to a lesser extent *in vivo*. Although there were no significant differences between the hAMSCs-Vector and hAMSCs-BMP4 treatment groups in regards to migration, proliferation, and differentiations *in vitro*, differences were noted *in vivo* with regards to GBM proliferation, nestin expression, and GBM migration (Table 1). Interestingly, hAMSCs-BMP4 and exogenous BMP4 can reduce migration and migration speed of BTICs, unlike the effect of BMP4 on other types of cancers (24-28). In addition, hAMSCs-BMP4 not only display tropism towards GBM tumor bulk, but can also home to migratory GBM cells *in vivo*. Most importantly, a single, cardiac injection of one million hAMSCs-BMP4 significantly increases survival of GBM-bearing mice compared to the hAMSCs-Vector and PBS treatments. Commercial GBM cell line U87 was used for the survival study because it is well-established and commonly used in GBM survival studies and has been shown to be extremely aggressive with a low survival rate, making it ideal to study survival in a murine GBM model (48-50). Future studies would be interested to use different subtypes of patient-

derived BTICs, including proneural, mesenchymal, classical, and neural, to perform survival studies and to investigate the molecular mechanisms behind the therapeutic effect of hAMSCs-BMP4. These studies will be a promising step towards personalized GBM therapy.

The present literature raises several additional concerns. The effects of cancer cells on the proliferative capacity and malignant potential of human MSCs is a critical consideration for its potential utility in clinical trials (9-11, 14). It has also been proposed that cancer cells may be able to induce MSCs to form tumor associated fibroblasts (TAFs), which can then support and stimulate tumor growth and migration as well as promote a malignant phenotype (18-20). We found that hAMSC proliferation does not increase in response to BTIC-secreted factors or co-culturing with BTICs *in vitro*. When cultured in conditioned media from BTICs *in vitro*, hAMSCs did not upregulate their expression of fibroblast markers suggesting that BTIC-hAMSC interaction does not foster the adoption of a TAF phenotype. *In vivo*, hAMSCs were not detectable 14 days after intracranial injection, suggesting that they are functional for only a short window of time. This has both advantages and disadvantages. The advantage of having this window of time is minimization of potential deleterious effects of cell therapy including oncogenesis, tumor induction, neovascularization, etc. The disadvantages include need for repeated cell injections, similar to chemotherapy. Despite the short window of time, however, a single cardiac injection of one million hAMSCs-BMP4 was able to significantly prolong survival of GBM-bearing mice. When injected alone and with BTICs, hAMSCs also did not demonstrate an increased proliferative capacity and no hAMSCs remained in the brain three months after injection. Furthermore, in our model of GBM, hAMSCs delivered to established tumors did not demonstrate co-localization with Ki67 and markers of tumor growth (TNF- $\alpha$  and VEGF) (51, 52) were attenuated in the presence of hAMSCs-BMP4. These results suggest that hAMSCs are neither tumor-supportive nor tumorigenic. In addition, we demonstrated that BTICs and BMP4 do not alter the stem cell properties, tumor tropism, or induce differentiation of hAMSCs in our experiments. Moreover, these cells retained their stem cell-like characteristics and tumor tropism *in vivo*, which is fundamental to their utility as a vehicle for anti-tumor agents. Two recent studies found that hAMSCs promoted growth and angiogenesis of GBM cells *in vivo* (53, 54). However, we discovered that hAMSCs-BMP4 decrease the proliferation of GBM cells, and hAMSCs-Vector and hAMSCs-BMP4 decrease the expression of the angiogenesis markers, VEGF and CD31 (data not shown) *in vivo*, although there was not sufficient quality and number of cells immunoreactive to CD31 to allow for quantification and statistical analyses. hAMSCs may therefore contribute to better outcomes in a multifactorial fashion, of which, angiogenesis is one component. Other components include tumor proliferation, migration, and differentiation, among others. Differences between our tumor models and those of Akimoto *et al.* in cell type, MSC source, injection site, and timing of MSC injections may account for these contrasting results. Notably, this prior study co-transplanted MSCs and GBM cells subcutaneously. Our experiments with intracranial injections were meant to be a proof the principle that ensured delivery of hAMSCs to the tumor mass and evaluate the safety of intracranial injection. We also delivered MSCs systemically through a single, cardiac injection to an established intracranial GBM tumor mass, which is thought to be a more accurate model for GBM in human patients.

In conclusion, our results demonstrate the extraordinary ability of hAMSCs-BMP4 to decrease the proliferative and migratory capacity of GBM cells, induce differentiation of BTICs *in vitro* and *in vivo*, and ultimately prolong survival GBM-bearing mice with a single, cardiac injection of one million cells. Additionally, our findings demonstrate the safety and efficacy of engineered hAMSCs in delivering targeted therapy in a mouse model of GBM. Both unmodified hAMSCs and hAMSCs-BMP4 do not undergo malignant transformation when exposed to GBM cells, and do not support tumor growth. Further advances with hAMSCs-BMP4 to create a more sophisticated delivery system may include engineering these cells to control the secretion of BMP4. TGF- $\beta$  and other markers specific to GBM cells within the brain (55, 56) may serve as molecular switches to induce the contextually specific release of BMP4. Based on our findings, we are optimistic that engineered hAMSC-based anticancer therapies will continue to demonstrate their promise in clinical trials for GBM. In the future, we predict this stem cell-based approach will have wide-reaching potential, including autologous hAMSCs from adipose tissue and the treatment of other primary and secondary brain cancers.

## Supplementary Material

Refer to Web version on PubMed Central for supplementary material.

## Acknowledgments

We thank Dr. K.H. William Lau from Loma Linda University for the gift of the BMP2/4 DNA plasmid, Bryant Beltran for designing the MATLAB program to track cells using the nanopattern assay, and Dr. Kenneth Aldape and Dr. Khalida Wani from the University of Texas MD Anderson Cancer Center for the GBM cell classification.

Grant supporting

This research was supported by the National Institutes of Health (RO1, NS070024) and the Maryland Stem Cell Research Fund (AQH).

## References

1. Stupp R, Mason WP, van den Bent MJ, Weller M, Fisher B, Taphoorn MJ, et al. Radiotherapy plus concomitant and adjuvant temozolomide for glioblastoma. *The New England journal of medicine*. 2005; 352:987–96. [PubMed: 15758009]
2. Quinones-Hinojosa A, Chaichana K. The human subventricular zone: a source of new cells and a potential source of brain tumors. *Experimental neurology*. 2007; 205:313–24. [PubMed: 17459377]
3. Bleau AM, Hambardzumyan D, Ozawa T, Fomchenko EI, Huse JT, Brennan CW, et al. PTEN/PI3K/Akt pathway regulates the side population phenotype and ABCG2 activity in glioma tumor stem-like cells. *Cell stem cell*. 2009; 4:226–35. [PubMed: 19265662]
4. Eramo A, Ricci-Vitiani L, Zeuner A, Pallini R, Lotti F, Sette G, et al. Chemotherapy resistance of glioblastoma stem cells. *Cell death and differentiation*. 2006; 13:1238–41. [PubMed: 16456578]
5. Murat A, Migliavacca E, Gorlia T, Lambiv WL, Shay T, Hamou MF, et al. Stem cell-related “self-renewal” signature and high epidermal growth factor receptor expression associated with resistance to concomitant chemoradiotherapy in glioblastoma. *Journal of clinical oncology : official journal of the American Society of Clinical Oncology*. 2008; 26:3015–24. [PubMed: 18565887]
6. Sakariassen PO, Immervoll H, Chekenya M. Cancer stem cells as mediators of treatment resistance in brain tumors: status and controversies. *Neoplasia*. 2007; 9:882–92. [PubMed: 18030356]
7. Strioga M, Viswanathan S, Darinkas A, Slaby O, Michalek J. Same or not the same? Comparison of adipose tissue-derived versus bone marrow-derived mesenchymal stem and stromal cells. *Stem cells and development*. 2012; 21:2724–52. [PubMed: 22468918]

8. Dominici M, Le Blanc K, Mueller I, Slaper-Cortenbach I, Marini F, Krause D, et al. Minimal criteria for defining multipotent mesenchymal stromal cells. The International Society for Cellular Therapy position statement. *Cytotherapy*. 2006; 8:315–7. [PubMed: 16923606]
9. Lamfers M, Idema S, van Milligen F, Schouten T, van der Valk P, Vandertop P, et al. Homing properties of adipose-derived stem cells to intracerebral glioma and the effects of adenovirus infection. *Cancer letters*. 2009; 274:78–87. [PubMed: 18842332]
10. Kosztowski T, Zaidi HA, Quinones-Hinojosa A. Applications of neural and mesenchymal stem cells in the treatment of gliomas. *Expert review of anticancer therapy*. 2009; 9:597–612. [PubMed: 19445577]
11. Lee DH, Ahn Y, Kim SU, Wang KC, Cho BK, Phi JH, et al. Targeting rat brainstem glioma using human neural stem cells and human mesenchymal stem cells. *Clinical cancer research : an official journal of the American Association for Cancer Research*. 2009; 15:4925–34. [PubMed: 19638465]
12. Xu F, Zhu JH. Stem cells tropism for malignant gliomas. *Neuroscience bulletin*. 2007; 23:363–9. [PubMed: 18064067]
13. Augello A, Kurth TB, De Bari C. Mesenchymal stem cells: a perspective from in vitro cultures to in vivo migration and niches. *European cells & materials*. 2010; 20:121–33. [PubMed: 21249629]
14. Momin EN, Mohyeldin A, Zaidi HA, Vela G, Quinones-Hinojosa A. Mesenchymal stem cells: new approaches for the treatment of neurological diseases. *Current stem cell research & therapy*. 2010; 5:326–44. [PubMed: 20528757]
15. Momin EN, Vela G, Zaidi HA, Quinones-Hinojosa A. The Oncogenic Potential of Mesenchymal Stem Cells in the Treatment of Cancer: Directions for Future Research. *Current immunology reviews*. 2010; 6:137–48. [PubMed: 20490366]
16. Kucerova L, Matuskova M, Hlubinova K, Altanerova V, Altaner C. Tumor cell behaviour modulation by mesenchymal stromal cells. *Molecular cancer*. 2010; 9:129. [PubMed: 20509882]
17. Nakamura K, Ito Y, Kawano Y, Kurozumi K, Kobune M, Tsuda H, et al. Antitumor effect of genetically engineered mesenchymal stem cells in a rat glioma model. *Gene therapy*. 2004; 11:1155–64. [PubMed: 15141157]
18. Spaeth EL, Dembinski JL, Sasser AK, Watson K, Klopp A, Hall B, et al. Mesenchymal stem cell transition to tumor-associated fibroblasts contributes to fibrovascular network expansion and tumor progression. *PloS one*. 2009; 4:e4992. [PubMed: 19352430]
19. Mishra PJ, Humeniuk R, Medina DJ, Alexe G, Mesirov JP, Ganesan S, et al. Carcinoma-associated fibroblast-like differentiation of human mesenchymal stem cells. *Cancer research*. 2008; 68:4331–9. [PubMed: 18519693]
20. Hall B, Dembinski J, Sasser AK, Studeny M, Andreeff M, Marini F. Mesenchymal stem cells in cancer: tumor-associated fibroblasts and cell-based delivery vehicles. *International journal of hematology*. 2007; 86:8–16. [PubMed: 17675260]
21. Pendleton C, Li Q, Chesler DA, Yuan K, Guerrero-Cazares H, Quinones-Hinojosa A. Mesenchymal Stem Cells Derived from Adipose Tissue vs Bone Marrow: In Vitro Comparison of Their Tropism towards Gliomas. *PloS one*. 2013; 8:e58198. [PubMed: 23554877]
22. Lee HK, Finnis S, Cazacu S, Bucris E, Ziv-Av A, Xiang C, et al. Mesenchymal stem cells deliver synthetic microRNA mimics to glioma cells and glioma stem cells and inhibit their cell migration and self-renewal. *Oncotarget*. 2013; 4:346–61. [PubMed: 23548312]
23. Altanerova V, Cihova M, Babic M, Rychly B, Ondicova K, Mravec B, et al. Human adipose tissue-derived mesenchymal stem cells expressing yeast cytosinedeaminase::uracil phosphoribosyltransferase inhibit intracerebral rat glioblastoma. *International journal of cancer Journal international du cancer*. 2012; 130:2455–63. [PubMed: 21732344]
24. Chiu CY, Kuo KK, Kuo TL, Lee KT, Cheng KH. The activation of MEK/ERK signaling pathway by bone morphogenetic protein 4 to increase hepatocellular carcinoma cell proliferation and migration. *Molecular cancer research : MCR*. 2012; 10:415–27. [PubMed: 22241220]
25. Guo D, Huang J, Gong J. Bone morphogenetic protein 4 (BMP4) is required for migration and invasion of breast cancer. *Molecular and cellular biochemistry*. 2012; 363:179–90. [PubMed: 22167620]

26. Deng H, Makizumi R, Ravikumar TS, Dong H, Yang W, Yang WL. Bone morphogenetic protein-4 is overexpressed in colonic adenocarcinomas and promotes migration and invasion of HCT116 cells. *Experimental cell research*. 2007; 313:1033–44. [PubMed: 17275810]
27. Virtanen S, Alarimo EL, Sandstrom S, Ampuja M, Kallioniemi A. Bone morphogenetic protein –4 and –5 in pancreatic cancer--novel bidirectional players. *Experimental cell research*. 2011; 317:2136–46. [PubMed: 21704030]
28. Braig S, Mueller DW, Rothhammer T, Bosserhoff AK. MicroRNA miR-196a is a central regulator of HOX-B7 and BMP4 expression in malignant melanoma. *Cellular and molecular life sciences : CMLS*. 2010; 67:3535–48. [PubMed: 20480203]
29. Piccirillo SG, Reynolds BA, Zanetti N, Lamorte G, Binda E, Broggi G, et al. Bone morphogenetic proteins inhibit the tumorigenic potential of human brain tumour-initiating cells. *Nature*. 2006; 444:761–5. [PubMed: 17151667]
30. Chaichana KL, Guerrero-Cazares H, Capilla-Gonzalez V, Zamora-Berridi G, Achanta P, Gonzalez-Perez O, et al. Intra-operatively obtained human tissue: protocols and techniques for the study of neural stem cells. *Journal of neuroscience methods*. 2009; 180:116–25. [PubMed: 19427538]
31. Guerrero-Cazares H, Chaichana KL, Quinones-Hinojosa A. Neurosphere culture and human organotypic model to evaluate brain tumor stem cells. *Methods Mol Biol*. 2009; 568:73–83. [PubMed: 19582422]
32. Colman H, Zhang L, Sulman EP, McDonald JM, Shooshtari NL, Rivera A, et al. A multigene predictor of outcome in glioblastoma. *Neuro-oncology*. 2010; 12:49–57. [PubMed: 20150367]
33. Peng H, Chen ST, Wergedal JE, Polo JM, Yee JK, Lau KH, et al. Development of an MFG-based retroviral vector system for secretion of high levels of functionally active human BMP4. *Molecular therapy : the journal of the American Society of Gene Therapy*. 2001; 4:95–104. [PubMed: 11482980]
34. Kang Y. Analysis of cancer stem cell metastasis in xenograft animal models. *Methods Mol Biol*. 2009; 568:7–19. [PubMed: 19582418]
35. Singh SK, Hawkins C, Clarke ID, Squire JA, Bayani J, Hide T, et al. Identification of human brain tumour initiating cells. *Nature*. 2004; 432:396–401. [PubMed: 15549107]
36. Tomita T, Akimoto J, Haraoka J, Kudo M. Clinicopathological significance of expression of nestin, a neural stem/progenitor cell marker, in human glioma tissue. *Brain tumor pathology*. 2013
37. Shah K. Mesenchymal stem cells engineered for cancer therapy. *Advanced drug delivery reviews*. 2012; 64:739–48. [PubMed: 21740940]
38. Garzon-Muvdi T, Schiapparelli P, ap Rhys C, Guerrero-Cazares H, Smith C, Kim DH, et al. Regulation of brain tumor dispersal by NKCC1 through a novel role in focal adhesion regulation. *PLoS biology*. 2012; 10:e1001320. [PubMed: 22570591]
39. Fuller GN. The WHO Classification of Tumours of the Central Nervous System. *Archives of pathology & laboratory medicine (4th edition.)*. 2008; 132:906. [PubMed: 18517270]
40. Erpolat OP, Akmansu M, Goksel F, Bora H, Yaman E, Buyukberber S. Outcome of newly diagnosed glioblastoma patients treated by radiotherapy plus concomitant and adjuvant temozolomide: a long-term analysis. *Tumori*. 2009; 95:191–7. [PubMed: 19579865]
41. Verhaak RG, Hoadley KA, Purdom E, Wang V, Qi Y, Wilkerson MD, et al. Integrated genomic analysis identifies clinically relevant subtypes of glioblastoma characterized by abnormalities in PDGFRA, IDH1, EGFR, and NF1. *Cancer cell*. 2010; 17:98–110. [PubMed: 20129251]
42. Nakamizo A, Marini F, Amano T, Khan A, Studeny M, Gumin J, et al. Human bone marrow-derived mesenchymal stem cells in the treatment of gliomas. *Cancer research*. 2005; 65:3307–18. [PubMed: 15833864]
43. Sasportas LS, Kasmieh R, Wakimoto H, Hingtgen S, van de Water JA, Mohapatra G, et al. Assessment of therapeutic efficacy and fate of engineered human mesenchymal stem cells for cancer therapy. *Proceedings of the National Academy of Sciences of the United States of America*. 2009; 106:4822–7. [PubMed: 19264968]
44. Alieva M, Bago JR, Aguilar E, Soler-Botija C, Vila OF, Molet J, et al. Glioblastoma therapy with cytotoxic mesenchymal stromal cells optimized by bioluminescence imaging of tumor and therapeutic cell response. *PloS one*. 2012; 7:e35148. [PubMed: 22529983]

45. Lim DA, Tramontin AD, Trevejo JM, Herrera DG, Garcia-Verdugo JM, Alvarez-Buylla A. Noggin antagonizes BMP signaling to create a niche for adult neurogenesis. *Neuron*. 2000; 28:713–26. [PubMed: 11163261]
46. Panchision DM, Pickel JM, Studer L, Lee SH, Turner PA, Hazel TG, et al. Sequential actions of BMP receptors control neural precursor cell production and fate. *Genes & development*. 2001; 15:2094–110. [PubMed: 11511541]
47. Westphal M, Lamszus K. The neurobiology of gliomas: from cell biology to the development of therapeutic approaches. *Nature reviews Neuroscience*. 2011; 12:495–508.
48. Martuza RL, Malick A, Markert JM, Ruffner KL, Coen DM. Experimental therapy of human glioma by means of a genetically engineered virus mutant. *Science*. 1991; 252:854–6. [PubMed: 1851332]
49. Menon LG, Kelly K, Yang HW, Kim SK, Black PM, Carroll RS. Human bone marrow-derived mesenchymal stromal cells expressing S-TRAIL as a cellular delivery vehicle for human glioma therapy. *Stem Cells*. 2009; 27:2320–30. [PubMed: 19544410]
50. Santra M, Zhang X, Santra S, Jiang F, Chopp M. Ectopic doublecortin gene expression suppresses the malignant phenotype in glioblastoma cells. *Cancer research*. 2006; 66:11726–35. [PubMed: 17178868]
51. van Horssen R, Ten Hagen TL, Eggermont AM. TNF-alpha in cancer treatment: molecular insights, antitumor effects, and clinical utility. *The oncologist*. 2006; 11:397–408. [PubMed: 16614236]
52. Ellis LM, Hicklin DJ. VEGF-targeted therapy: mechanisms of anti-tumour activity. *Nature reviews Cancer*. 2008; 8:579–91.
53. Akimoto K, Kimura K, Nagano M, Takano S, To'a Salazar G, Yamashita T, et al. Umbilical Cord Blood-Derived Mesenchymal Stem Cells Inhibit, But Adipose Tissue-Derived Mesenchymal Stem Cells Promote, Glioblastoma Multiforme Proliferation. *Stem cells and development*. 2013
54. Akimoto K, Kimura K, Nagano M, Takano S, Salazar G, Yamashita T, et al. Umbilical cord blood-derived mesenchymal stem cells inhibit, but adipose tissue-derived mesenchymal stem cells promote glioblastoma multiforme proliferation. *Stem cells and development*. 2012
55. Penuelas S, Anido J, Prieto-Sanchez RM, Folch G, Barba I, Cuartas I, et al. TGF-beta increases glioma-initiating cell self-renewal through the induction of LIF in human glioblastoma. *Cancer cell*. 2009; 15:315–27. [PubMed: 19345330]
56. Wu A, Wei J, Kong LY, Wang Y, Priebe W, Qiao W, et al. Glioma cancer stem cells induce immunosuppressive macrophages/microglia. *Neuro-oncology*. 2010; 12:1113–25. [PubMed: 20667896]

### Translational Relevance

Glioblastoma (GBM) is the most common primary intracranial malignant cancer in adults, and is associated with poor outcomes despite multimodality therapy. This lack of effectiveness of current therapies is presumably due to a small subset of tumor cells, so called brain tumor initiating cells (BTICs), with self-renewal capabilities and stronger tumor initiating capacities. Mesenchymal stem cells (MSCs) have an endogenous tropism towards certain cancers, and adipose tissue provides a feasible and less invasive source of MSCs. Moreover, bone morphogenetic protein (BMP4) has been shown to decrease proliferation by inducing BTIC differentiation. Therefore, adipose-derived MSCs engineered to secrete BMP4 (hAMSCs-BMP4) may be a potential effective treatment option for GBM. In this study, we show that engineered hAMSC-BMP4 cells reduce the proliferation and migration of GBM and induce differentiation of BTICs *in vitro* and *in vivo*. Furthermore, a single, cardiac injection of these cells into a mouse model of GBM significantly prolongs survival. These findings suggest that hAMSCs-BMP4 are a promising novel cell-based therapy for patients with GBM and potentially other metastatic cancers.



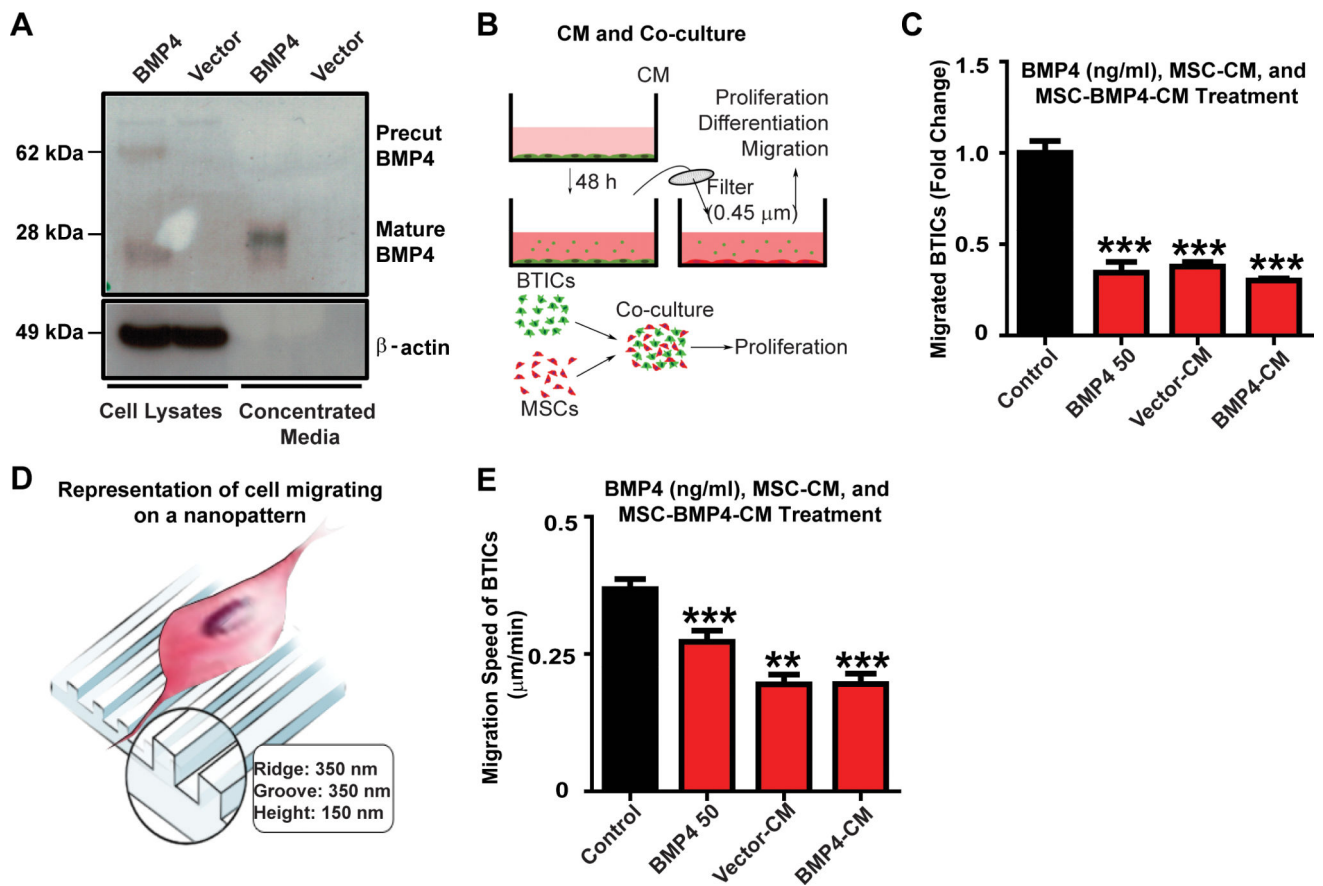


**Figure 1. hAMSCs-BMP4 decrease migration of BTICs *in vitro***

(A) hAMSCs were infected with BMP4 or vector retroviruses. Western blots were performed using cell lysates and concentrated media.  $\beta$ -actin served as a loading control. (B) Schematic of conditioned media (CM) collection and co-culturing methods. (C) BTICs were treated with 50 ng/ml BMP4, or were cultured in hAMSC-Vector-CM, hAMSC-BMP4-CM, or control media for 24 hours and a Boyden transwell assay was performed. Results were normalized and compared to the control media condition. (D) Schematic of cells migrating on a nanopattern. (E) Nanopattern assay of BTICs cultured in hAMSC-Vector-CM, hAMSC-BMP4-CM, control media, or treated with 50 ng/ml BMP4. \* $p < 0.05$ , \*\* $p < 0.01$ , \*\*\* $p < 0.001$ .

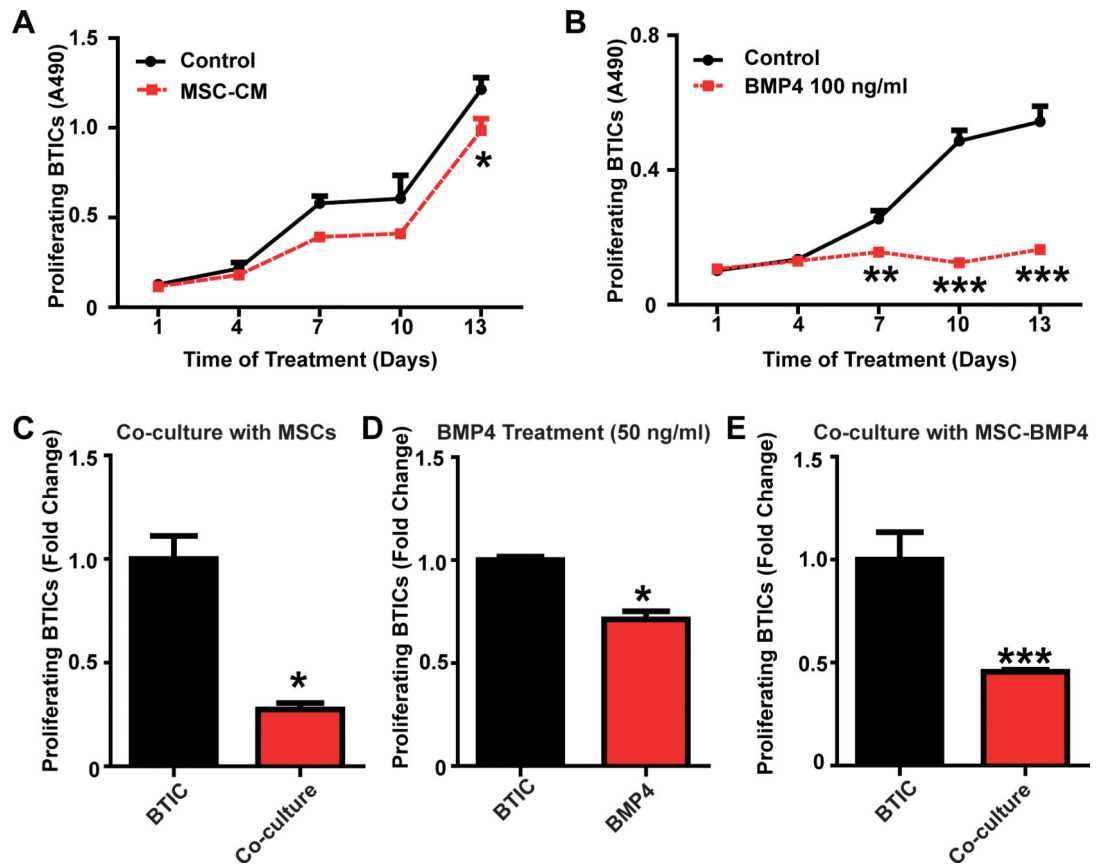


**Figure 2. hAMSCs-BMP4 decrease BTIC proliferation *in vitro***

BTICs were cultured in (A) hAMSC-CM or (B) BMP4 treated media (100ng/ml) for 2 weeks, and MTS assays were performed to measure BTIC proliferation. EdU assay of GFP-BTICs (C) co-cultured with hAMSCs for 5 days, (D) treated with BMP4 (50 ng/ml) for 48 hours, or (E) co-cultured with hAMSCs-BMP4 for 5 days to determine the proliferation of BTICs. Results were normalized and compared to BTICs condition. \* $p < 0.05$ , \*\* $p < 0.01$ , \*\*\* $p < 0.001$ .

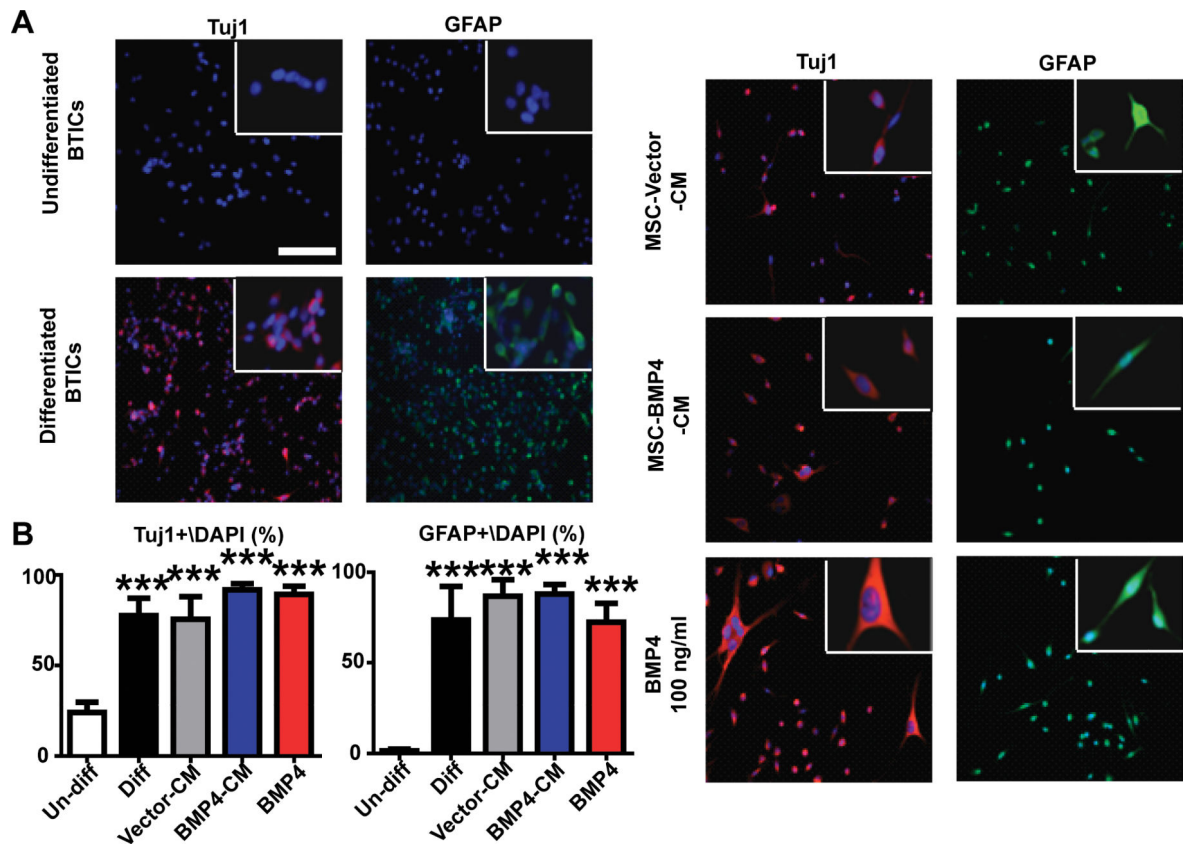


**Figure 3. hAMSCs-BMP4 promote BTIC differentiation *in vitro***

(A) BTICs were cultured in control media (stem cell media, undifferentiated BTICs), differentiation media (stem cell media+10%FBS, differentiated BTICs), hAMSC-Vector-CM, hAMSC-BMP4-CM, or BMP4 (100 ng/ml) for 2 weeks and immunofluorescence staining for Tuj1 and GFAP was performed, with magnification in the upper right insets. Scale bar, 200  $\mu$ m. (B) The percentages of Tuj1+/DAPI and GFAP+/DAPI were calculated from 5 random fields for the different conditions. \*\*\* $p < 0.001$ .

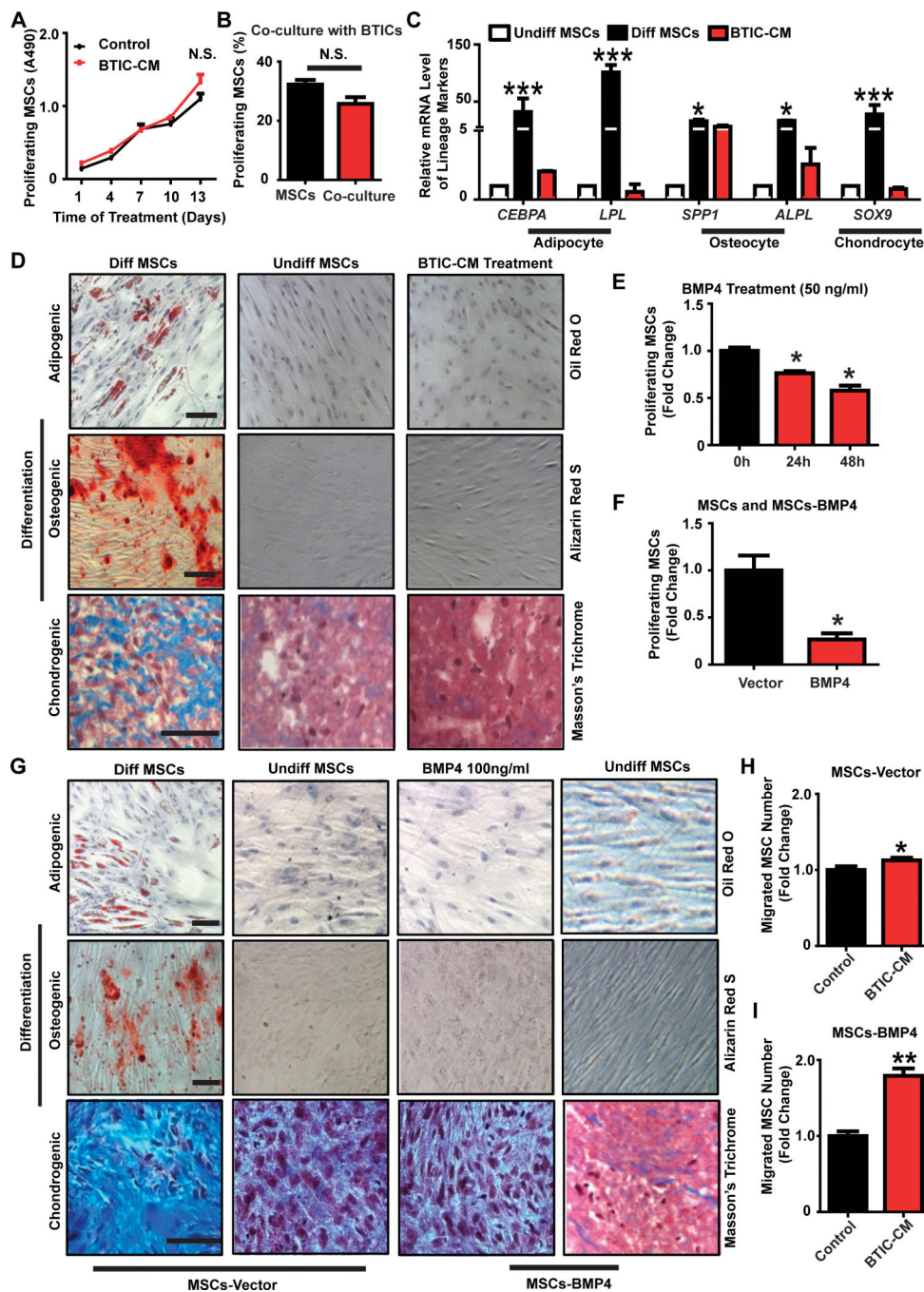


**Figure 4. hAMSCs remain multipotent and retain proliferation capacity when exposed to BTIC-CM or transduced with BMP4 *in vitro***

(A) MTS assay of hAMSCs cultured in BTICCM or control media for 2 weeks to measure proliferating hAMSCs every 3 days. (B) EdU assay of td-tomato-hAMSCs co-cultured with BTICs for 5 days to determine proliferating hAMSCs. (C) Real-time RT-PCR was performed. Markers for adipocyte, osteocyte and chondrocyte lineages were tested. GAPDH served as a control. Other groups were normalized and compared to the undifferentiated hAMSCs group. (D) hAMSCs were cultured in control media (undifferentiated hAMSCs), differentiation media (differentiated hAMSCs), or BTIC-CM for 3 weeks. Various stains

were performed to assess differentiation capabilities (scale bar, 100  $\mu\text{m}$ ) and (E) EdU assay of hAMSCs treated with BMP4 (50 ng/ml) for different time periods (24 hours and 48 hours) to measure hAMSC proliferation. Results were normalized and compared to the 0 hour condition. (F) EdU assay comparing proliferation of hAMSCs-Vector and hAMSCs-BMP4 cells after 5 days of culturing. Results were normalized and compared to hAMSCs-Vector. (G) hAMSCs-Vector, hAMSCs-Vector treated with BMP4 (100 ng/ml), or hAMSCs-BMP4 cultured in control media or differentiation media for 3 weeks. Various lineage stains were performed as described previously. Scale bar, 100  $\mu\text{m}$ . (H-I) Transwell assays: hAMSCs-Vector (H) or hAMSCs-BMP4 (I) were seeded on top chamber. BTIC-CM or control media+2% FBS was at the bottom of the chamber. Results were normalized and compared to control.\* $p$ <0.05, \*\* $p$ <0.01, \*\*\* $p$ <0.001; N.S., not significant.

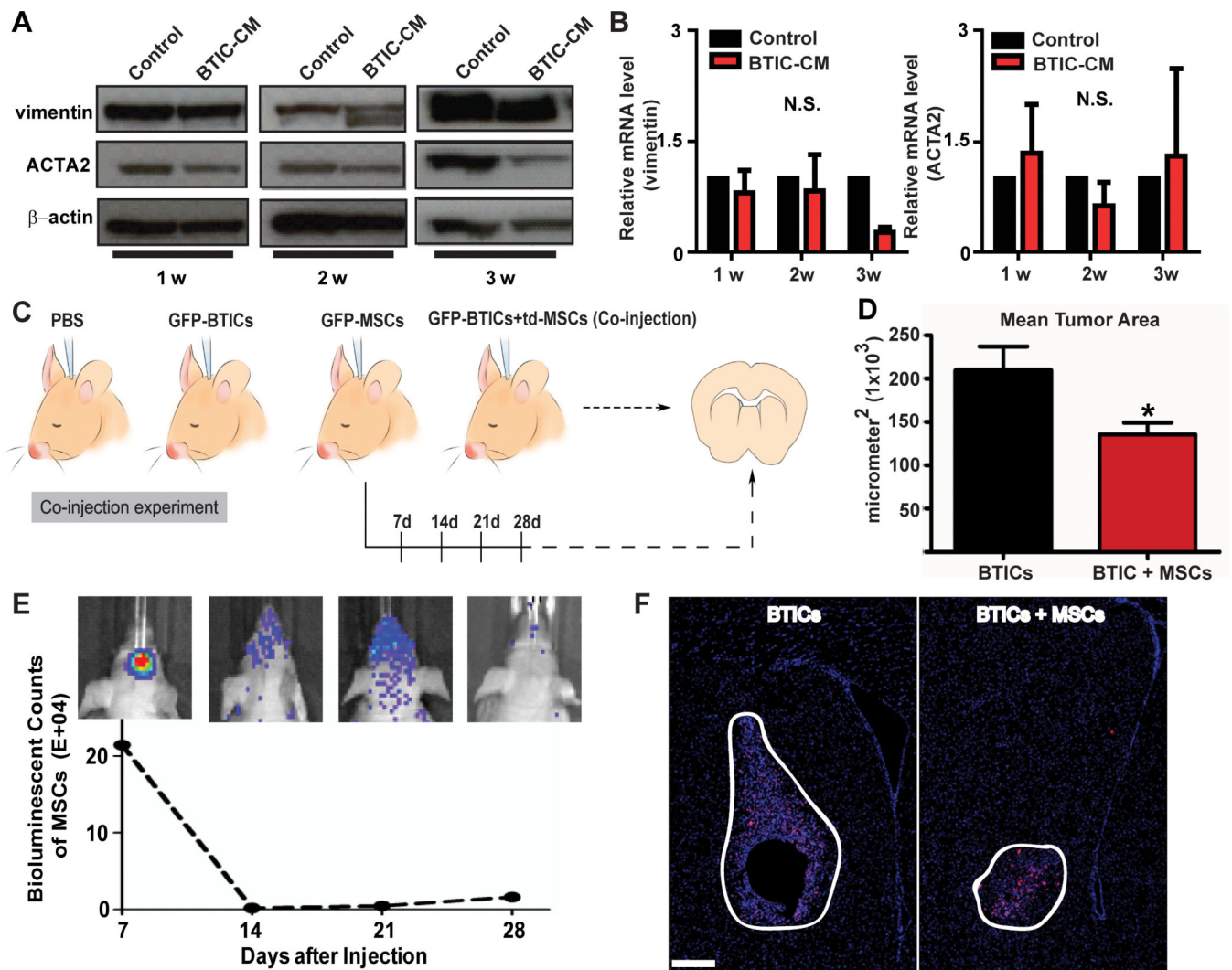


**Figure 5. hAMSCs are not tumorigenic and do not transform into tumor associated fibroblasts (TAFs) *in vitro* or *in vivo***  
 (A-B) hAMSCs were cultured in BTIC-CM or control media for 1-3 weeks and (A) Western blots ( $\beta$ -actin served as a control) and (B) Real-time RTPCR (GAPDH served as a control) were performed to quantify TAF markers (vimentin and ACTA2). (C) Schematic of the co-injection experiment where PBS, GFP-BTICs, GFP/bioluminescent-hAMSCs (GFP-hAMSCs), or GFP-BTICs mixed with td-tomato-hAMSCs (td-hAMSCs) were injected into mice and sacrificed and sacrificed 4 weeks later. (D) Quantification of mean tumor area of the GFP-BTIC and co-injection groups using DAPI staining. The co-injection group had a smaller mean tumor area of  $135,700 \mu\text{m}^2$  as compared to GFP-BTIC group, with a mean tumor area of  $209,800 \mu\text{m}^2$  ( $p=0.0189$ ). (E) Live animal imaging of the GFP-hAMSCs condition. At 14 days post GFP-hAMSCs injection, the hAMSC signal drastically decreases. Each mouse brain represents the counts of bioluminescent signal at each time point. (F) DAPI and human nuclei stain for GFP-BTICs and co-injection groups ( $n=5$ ). Larger tumors were only seen in the GFP-BTICs condition compared the co-injection condition. Brain sections and tumor mass are outlined. Scale bar,  $200 \mu\text{m}$ . N.S., not significant.

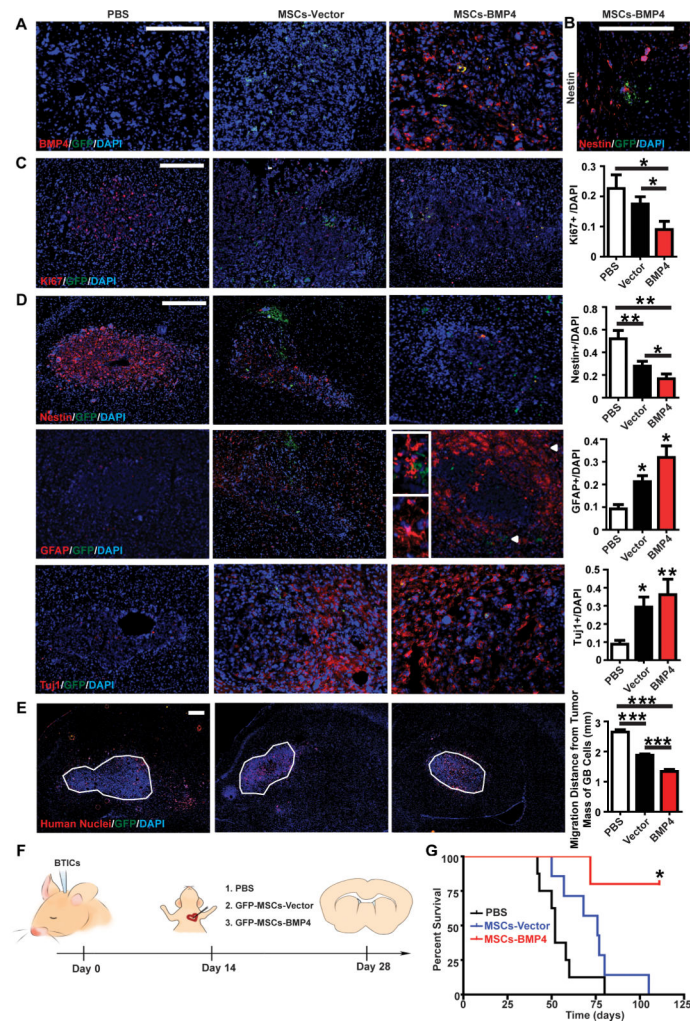


**Figure 6. hAMSCs-BMP4 increase the median survival time of GBM bearing mice, drive differentiation, and decrease proliferation and migration of GBM cells *in vivo***  
 (A) Immunoreactivity for GFP and BMP4 to test the expression of BMP4. Scale bars, 200  $\mu$ m. (B) GFP-hAMSCs-BMP4 cells were seen near satellite Nestin<sup>+</sup> cells away from the main tumor bulk. Scale bars, 200  $\mu$ m. (C) Representative pictures and quantification of GFP and Ki67 staining to test the proliferation of GBM cells. Scale bars, 200  $\mu$ m. (D) Representative pictures and quantification of GFP, Nestin, GFAP, and Tuj1 staining to test the differentiation of BTICs. Arrowheads in the GFP-hAMSC-BMP4 GFAP staining correspond to magnified insets of GFP-hAMSC-BMP4 and GFAP<sup>+</sup> cells at the tumor center, and a GFAP<sup>+</sup> cell with mature astrocytic morphology at the tumor periphery. Magnified pictures are shown on the left. Scale bars, 200  $\mu$ m. (E) Representative pictures (right hemisphere) and quantification of migratory GBM cells. The average distance of migrated GBM cells, identified as human nuclei<sup>+</sup>/DAPI<sup>+</sup>/GFP<sup>-</sup> cells outside tumor bulk, from the center of tumor mass (outlined) was measured. Scale bars, 200  $\mu$ m. \* $p$ <0.05, \*\* $p$ <0.01, \*\*\* $p$ <0.001. (F) Schematic of the *in vivo* experiment for which immunofluorescence staining was performed in panels A-E: BTIC culture 276 were intracranially injected into 6-8 week-old nude mice. At 4 weeks post-

injection, GFP-hAMSCs-Vector (n=7), GFP-hAMSCs-BMP4 (n=5), or equal volumes of PBS (n=5) were injected intracardially. Mice were sacrificed 2 weeks later. (G) U87 cells were intracranially injected into 6-8 week-old nude mice. Ten days post-injection, GFP-hAMSCs-Vector (n=7), GFP-hAMSCs-BMP4 (n=5), or equal volumes of PBS (n=10) were injected intracardially. Mice were followed for 125 days to monitor survival. Kaplan-Meier survival analysis resulted in the median survival of mice treated with hAMSCs-BMP4 (undefined) was significantly greater than that of mice treated with hAMSCs-Vector (p=0.01) (76 days) and control mice (p=0.002) (52 days), with no significant difference between the PBS and hAMSCs-Vector group (p=0.09).



**Table 1**

Summary of hAMSCs and hAMSCs-BMP4 Effects on BTICs

	BTIC Behavior	Control Condition vs.		hAMSC treatment vs. hAMSC-BMP4 treatment
		hAMSC treatment	hAMSC-BMP4 treatment	
<i>In Vitro</i>	Proliferation	*	*	N.S.
	Differentiation	*	*	N.S.
	Migration/Migration Speed	*	*	N.S.
<i>In Vivo</i>	Proliferation	*	*	*
	Differentiation	*	*	*
	Migration	*	*	*
	Survival	N.S.	*	*

\* represents statistical significance,  $p < 0.05$ ; N.S. represents no significance,  $p > 0.05$